TECHNION
Israel Institute of Technology

BME Faculty of Biomedical Engineering

ANNUAL PROJECTS SHOWCASE

ABSTRACTS BOOKLET

Where BioMedical ideas come to life

20.07.2026

Book of Abstracts

Dear all,

We are proud and honored to welcome you to take part in the: ***Annual Project Presentation Conference 2025 of the Biomedical Engineering Faculty***.

This meeting culminates a yearlong research and development experience for our 4th year students. There is a say in Hebrew tradition: "אין חכם כבעל ניסיון", meaning "Experience brings wisdom". This, in a nutshell, is what the projects are all about.

During their project development experience, our students had to undergo through all the stages needed to make an idea come true. Starting with a medical problem which they had to tackle, they had to strain their imagination and think "out of the box" in order to come up with a plausible new solution. Then, they had to combine the knowledge they gained during their studies. This knowledge encompasses all the aspects of biomedical engineering, i.e. combining medical background with engineering skills and scientific knowledge. All this package had to be implemented in order to provide a real-world solution.

We believe that this hands-on experience exposed and prepared our graduates to the High-Tech biomedical industry and to a wide variety of biomedical research in a very strong way encouraging multidisciplinary work that is vital for the students' future career, and in addition potentially foster their entrepreneurship skills.

In this booklet the abstracts of all presented projects are displayed for your perusal. We are sure that the students are eager to present the outcome of their year-long projects. We wish all of them rewarding careers after graduation. We hope that very soon they will take an active part in similar projects as professional mentors from both industry and academia.

We look forward to this year's event hosted at the Technion's Visitors Center.

Kindest Regards,

Prof. Josué Sznitman, Faculty Dean

Dr. Arielle G. Fischer, Course Instructor

Project 1

A Novel Non-Invasive System for Early Detection and Monitoring of Heart Failure Decompensation Through Quantitative Analysis of Respiratory Dynamics

Chen Lerman[1], Snir Rozner[1], Lior Segal[1], Nevo Stern[1], Amit Parizat[1], Nisim Vatury[2], Amir Landsberg[1,2]
[1] Faculty of Biomedical Engineering, Technion – Israel Institute of Technology, Haifa, Israel
[2] Levron Medical Ltd.

Introduction: Acute heart failure deterioration affects millions worldwide and is the leading cause of rehospitalization. Current monitoring approaches detect deterioration too late, leading to preventable hospitalizations and poor patient outcomes. While existing tools focus on tracking fluid accumulation (late detection) or internal pressures (invasive), no current technology monitors or quantifies the symptom that patients complain about and can detect subclinical signs of decompensation. To bridge this gap, this project aims to achieve a paradigm shift: "From Subjective Symptom to Objective Sign". The primary objective is to develop and validate a non-invasive, low-cost, tri-axial accelerometer system designed to capture early signs of decompensation by directly quantifying respiratory effort dynamics.

Methods: Systematic bench calibration of the accelerometer device was performed first, followed by human experiments with the sensor secured on the patient's epigastrium. The signals were validated by isolating key physiological landmarks and correlating them with clinical airflow mask data. From the accelerometer signal, we extracted two key respiratory effort metrics: the inspiration-to-expiration time ratio (I:E) and the Excessive Effort Index (EEI). Crucially, the EEI extracts high-frequency spectral power distributions via Welch's method, capturing entirely new clinical information regarding accessory muscle recruitment that cannot be extracted from airflow measurements. These parameters were calibrated using a sigmoidal curve to suppress baseline physiological noise while capturing pathological trends. The system was evaluated across 6 healthy control subjects at rest and heavy breathing, alongside 7 heart failure patients assessed before, during, and after Levron's clinical treatment.

Results: The correlation between epigastric kinematics and the airflow was confirmed, demonstrating a stable physiological phase delay between chest wall displacement and air volume exchange. The composite distress score achieved clean clinical classification. For healthy subjects, the model successfully suppressed baseline noise (1.2 ± 2.6), while accurately capturing elevated effort during heavy breathing ($66.6 \pm 26.3, p = 0.0375$). Conversely heart failure patients at rest demonstrated elevated clinical distress scores (52.9 ± 23.5) showing a high contrast from healthy controls ($p = 0.0006$). Following medical treatment, the composite distress index dynamically tracked recovery within minutes, confirming the system's sensitivity to changing physiological states.

Conclusions: This project demonstrates that a non-invasive, home-targeted system for monitoring the respiratory dynamics can reliably transform the subjective symptom of dyspnea into quantifiable clinical signs. Integrating the EEI and I:E ratios into a joint sigmoidal calibration curve successfully filters out healthy baseline noise while maintaining high sensitivity to pathological changes. The clinical and commercial utility should be further evaluated in a large clinical trial.

Keywords: Heart Failure deterioration, Tri-Axial Accelerometer, Respiratory Effort.

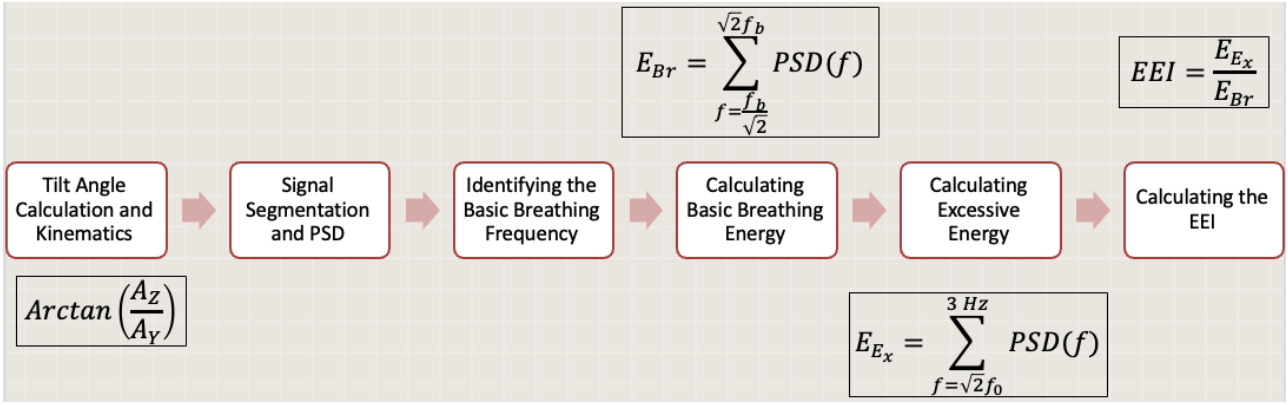

Figure 1. *The EEI pipeline: Epigastric tilt is derived via accelerometer axes, segmented and transformed using Welch's power spectral density. The algorithm isolates basic breathing energy (E_{Br}) around the dominant breathing frequency (f_b) and quantifies high-frequency recruitment (E_{Ex}) to extract the final EEI ratio.*

Project 2

Guardrail-Based Safety and Reliability Enhancement of a Medical Instructions for Use Chatbot

Einav Cohen[1], Moran Ohana[1], Shani Menahem[1], Kfir Hadar[1], Anat Rotschild[1] and Irit Ben-Avraham[2]
[1] Faculty of Biomedical Engineering, Technion - Israel Institute of Technology, Haifa, Israel
[2] Philips Healthcare, Haifa, Israel

Introduction: Medical information chatbots that retrieve content from official Instructions for Use documents can improve access to complex product guidance. However, the use of generative artificial intelligence in a medical context requires additional mechanisms to ensure that responses remain accurate, complete, and appropriately grounded in the available documentation. This project aimed to improve the safety, reliability, and response quality of the Philips Smart Search assistant for Advanced Visualization Workspace by integrating targeted guardrails into the existing retrieval-based system.

Methods: Five guardrails were integrated in two stages. Three prompt-level guardrails addressed object mismatch, broad or ambiguous questions, and insufficient workflow evidence during response generation. Two post-answer guards operated before display: a measurement-reliability guard added required reliability conditions for quantitative cardiac measurements only when absent, and a warning and caution guard detected safety items retrieved from the Instructions for Use documents but omitted from the response. A central runner coordinated the guardrails and recorded validation metadata. The integrated workflow was executed across 50 active validation cases. In addition, each guardrail family was evaluated using a dedicated targeted question set designed to test its specific objective. For the deterministic post-answer guards, the actual action was compared with a predefined expected action. For the response-quality guardrails, each chatbot response was compared with its corresponding ground-truth answer using an automated AnswerCorrectness metric, and paired scores were compared before and after guardrail activation.

Results: The integrated pipeline completed all 50 validation cases successfully. Measurement-reliability actions matched expectations in 11 of 11 targeted cases: required disclosures were present in all 5 positive cases, and all 6 negative or near-miss cases correctly remained unchanged. The warning and caution guard flagged missing safety items in 9 of 9 targeted cases. Across 12 paired response-quality cases, mean AnswerCorrectness increased from 0.4577 to 0.6253, an absolute increase of 0.1676 and a relative improvement of 36.6%; 9 of 12 cases improved.

Conclusions: The integrated framework reliably applied safety and measurement-reliability checks before the final response was shown and demonstrated a positive trend in response quality across targeted failure scenarios. Separating guardrails by failure type and validation objective provides a practical, modular strategy for strengthening Instructions for Use chatbots while preserving the underlying retrieval and generation pipeline.

Keywords: medical chatbot; guardrails; clinical artificial intelligence; Instructions for Use

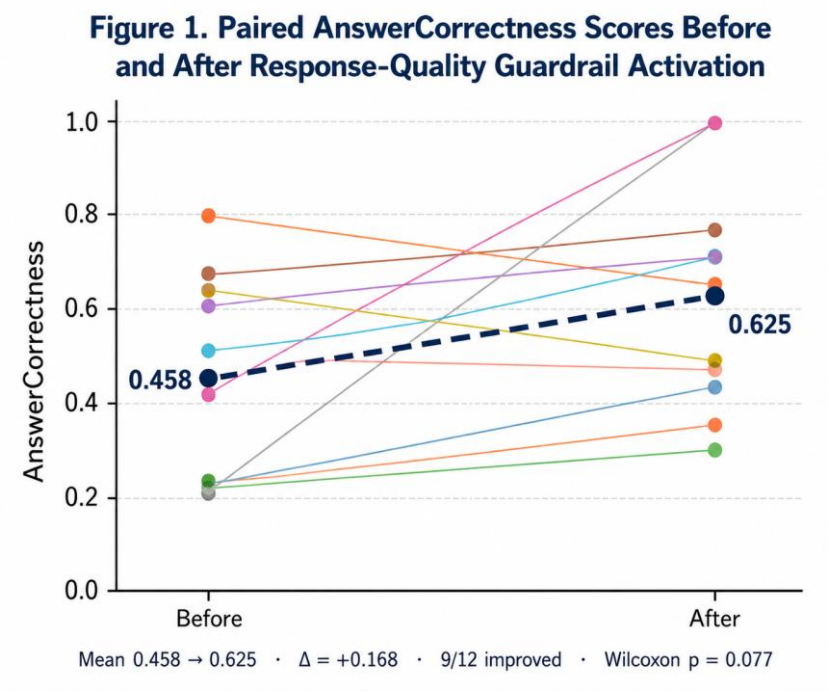

Figure 1. *Paired AnswerCorrectness scores before and after response-quality guardrail activation. Mean scores increased from 0.458 to 0.625, with 9 of 12 cases improving (Wilcoxon signed-rank test, p = 0.077).*

Project 3

Development of an Automated Tool for Synthetic Image Quality Control

Yarden Fainzilber[1], Sivan Friedrich[1], Mor Lev[1], Yuval Naim[1], Ofir Oren[1], Sofia Orlov[1], Anat Rotschield[1], Dan Shahak[2] and Irit Ben-Avraham[2]
[1] Faculty of Biomedical Engineering, Technion - Israel Institute of Technology, Haifa, Israel
[2] Philips Healthcare, Haifa, Israel

Introduction: Training deep learning models for medical imaging requires large datasets. However, acquiring real patient scans is challenging due to high costs, privacy concerns, and limited population representation. While synthetic data generation addresses this limitation, generated images may contain subtle anatomical inconsistencies that are difficult to detect manually. Such data may lead models to learn unrealistic anatomical or radiomic patterns, reducing their clinical reliability. This project presents a fully automated framework for assessing synthetic Computed Tomography images, providing organ-level evaluation and an overall realism score before model training.

Methods: The framework consists of a multi-stage validation pipeline for evaluating synthetic Computed Tomography images. The first validation gate compares organ size, center of mass, and inter-organ distances with reference ranges derived from real Computed Tomography images. Images with more than two anatomical deviations are rejected. For the remaining images, sixty-three radiomic features from the Shape, First-Order, and Gray-Level Co-occurrence Matrix (GLCM) families were extracted from five target organs, including features computed from wavelet-filtered images. The second validation gate applies Mahalanobis distance to identify statistically inconsistent multivariate radiomic feature relationships. Only images passing both validation gates proceed to the final scoring stage, where Kernel Density Estimation models the probability density of each radiomic feature using the reference distribution of real data. Feature scores are aggregated into organ-level and overall image realism scores.

Results: The pipeline was evaluated using 704 real and 83 synthetic Computed Tomography scans. The anatomical validation gate rejected six synthetic outliers, while the Mahalanobis validation gate identified one additional statistically inconsistent image. Images passing both stages received a realism score between 0 and 1, where higher scores indicate greater similarity to real CT distributions. Using an acceptance threshold of 0.8, three additional images were rejected, resulting in 10 of 83 synthetic images failing the framework. All synthetic images were evaluated through every stage to assess framework consistency. An expert radiologist validated the complete pipeline, confirming that decisions at each validation stage and the final realism scores were consistent with clinical assessment.

Conclusions: This project presents a multi-stage framework that combines anatomical validation, radiomics, and statistical modeling to evaluate the realism of synthetic Computed Tomography images. The framework provides an objective and quantitative quality assessment

that was validated by an expert radiologist, enabling reliable selection of synthetic data for deep learning model training.

Keywords: Synthetic Computed Tomography, Quality Assessment, Radiomics, Kernel Density Estimation

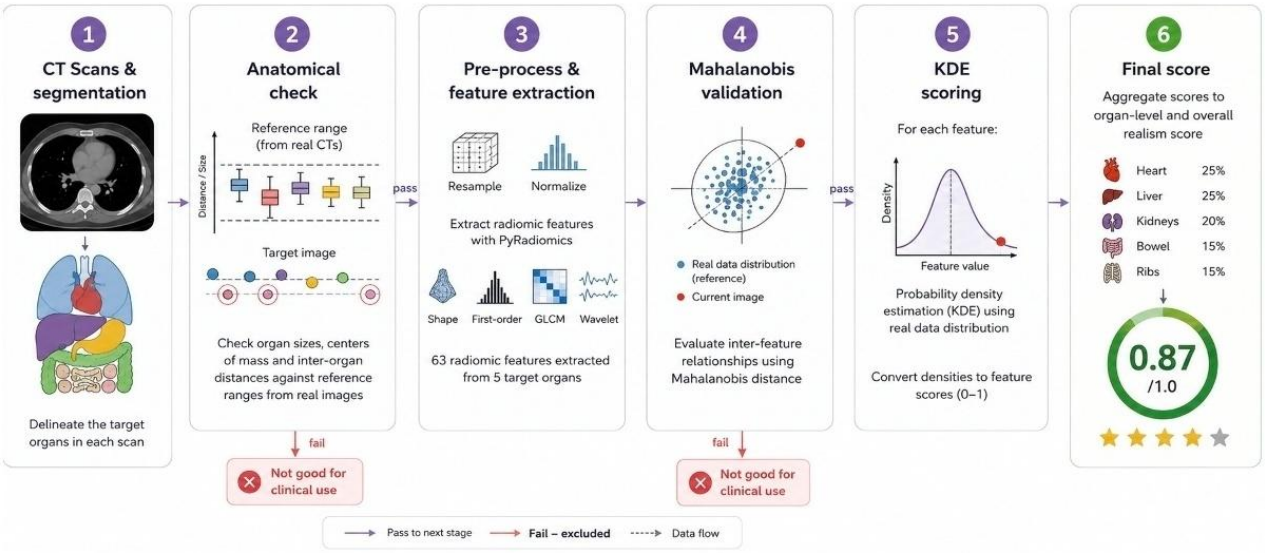

***Figure 1**. Overview of the proposed multi-stage framework for evaluating the realism of synthetic Computed Tomography images. The pipeline combines anatomical validation, radiomics-based statistical validation, and Kernel Density Estimation scoring to generate an objective organ-level and overall image realism score.*

Project 6

A Three-Dimensional Preterm Airway Model For Quantifying Surfactant Distribution

Lara Abu Nassar [1], Adan Daher[1], Clara Jammal[1], Nai Khoury[1], Aleen Meika[1], Daniel Katz[1], Ron Bessler[1],Dana Amit[1],Oshri Farhana[1] and Josue Snitzman[1]

[1] Faculty of Biomedical Engineering, Technion - Israel Institute of Technology, Haifa, Israel

Introduction: Surfactant therapy is one of the most important treatments for premature infants suffering from respiratory distress syndrome, yet no routine method currently exists to quantify how surfactant spreads inside the lungs after administration. Although surfactant distribution is known to be non-uniform, the stage along the airway at which this asymmetry begins remains unclear. Identifying where the asymmetry originates may clarify the underlying distribution mechanism and support strategies to improve it. The objective of this project was to develop a transparent, anatomically based, three-dimensionally printed model of the neonatal airway that enables controlled, quantitative measurement of surfactant distribution, and to establish a platform for future evaluation of intrapulmonary percussive ventilation as a means of improving distribution uniformity.

Methods: An anatomical model of the first four generations of a preterm airway was designed from computed tomography data while preserving branch lengths, bifurcation angles, and diameters. A hollow, transparent airway replica was fabricated by sacrificial molding. A water-soluble inner core made from butanediol vinyl alcohol co-polymer was printed with integrated support walls, embedded in polydimethylsiloxane, and dissolved after curing to obtain a sealed structure with eight outlet branches. Each outlet was connected to a collection tube for measuring the delivered fluid volume. A breathing simulator generated inspiration and expiration cycles representing preterm respiratory conditions. Airflow was recorded and synchronized with the respiratory cycle to obtain the full respiratory waveform, and a fixed volume of surfactant analogue was injected under identical ventilation conditions. The collected volume from each outlet was measured across seven repeated trials to evaluate distribution symmetry and reproducibility.

Results: Seven repeated experiments were performed under identical ventilation and injection conditions. As shown in **Figure 1**, surfactant analogue distribution among the eight outlets was consistently non-uniform across all experiments. Outlets 5–8, which belong to one side of the first airway bifurcation and correspond anatomically to the left lung, collected larger fluid volumes than outlets 1–4, which correspond to the right lung. This reproducible bias was observed despite variability in the absolute volumes collected at each outlet. These results indicate that surfactant distribution asymmetry already exists at the level of the first bifurcation, rather than emerging only in more distal airway generations.

Conclusions: Simulated intratracheal surfactant delivery under the tested conditions resulted in non-uniform distribution across the proximal preterm airway, with asymmetry traced back to the first bifurcation rather than distal generations. The developed three-dimensional airway model enables quantitative, repeatable assessment of surfactant distribution and supports future

controlled testing of intrapulmonary percussive ventilation to determine whether active pulsatile airflow improves distribution compared with standard delivery.

Keywords: Preterm Infants, Surfactant Distribution, Neonatal Airway Model, Intrapulmonary Percussive Ventilation

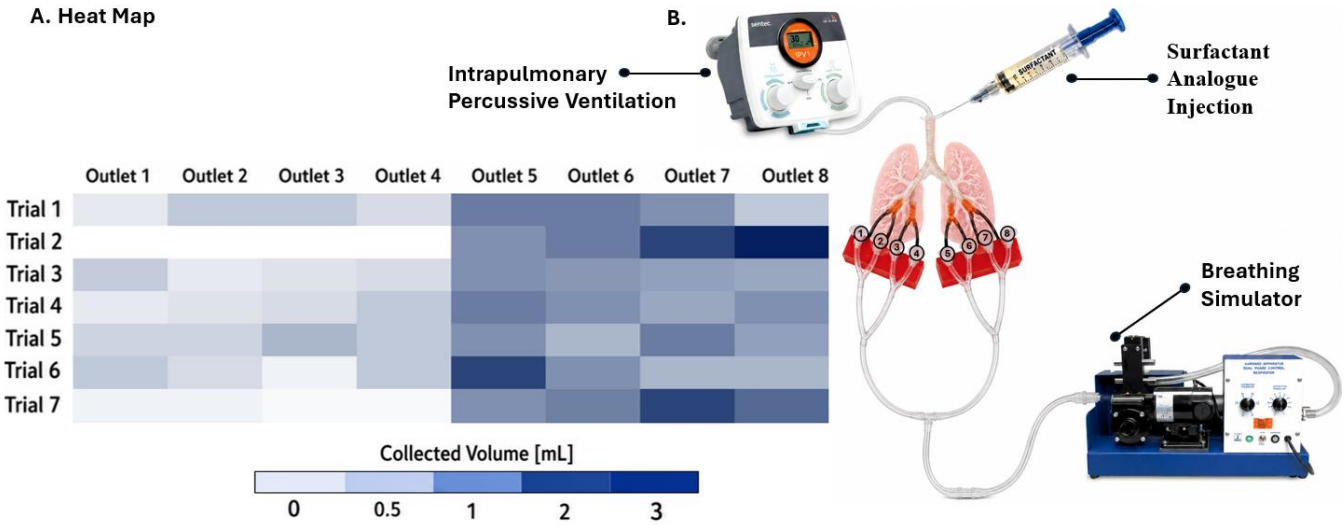

Figure 1. *Experimental platform and surfactant analogue distribution results.* ***A:*** *Heat map of collected surfactant analogue volume across eight outlets over seven repeated experiments, showing reproducible non-uniform distribution.* ***B:*** *Experimental setup including the preterm airway model, surfactant analogue injection, breathing simulator, and intrapulmonary percussive ventilation device for future controlled testing.*

Project 7

Innovative Bioreactor For Engineered Vessel Maturation And Monitoring

Basim Qraqra[1], Ruth Tshuva[1], Ofek Kleinberger[1], Rjaa Kadah[1], Michal Turgeman[1], Maya Yaakov-Jakubovitz[1], Tom Blechman[1], Daniel Katz[1] and Shulamit Levenberg[1]

[1] Faculty of Biomedical Engineering, Technion – Israel Institute of Technology, Haifa, Israel

Introduction: Tissue engineering seeks to develop functional living tissues in vitro that closely replicate the structural and physiological properties of native human tissues. Blood vessel engineering remains a key element in tissue engineering, since most organs rely on an intact vascular network for the supply of nutrients and the clearance of metabolic waste. Engineered blood vessels require a well-defined three-dimensional scaffold, along with a controlled biological environment and physiologically relevant fluid flow provided by a bioreactor to promote proper tissue development. However, many existing bioreactor systems are large, costly, complex to operate, not specifically tailored for vascular constructs, and most importantly, limited in their ability to provide direct real-time visualization. Therefore, the objective of this project was to design and develop a compact, transparent, and accessible bioreactor system that enables controlled flow, supports engineered blood vessel maturation, and allows continuous real-time monitoring.

Methods: The project was divided into three main parts: scaffold development, bioreactor design, and connection between the soft scaffold and the external tubing system. The scaffold was fabricated as a hollow U-shaped blood vessel tube using injection molding, composed of a two-piece mold, a dissolvable insert, and an injected hydrogel mixture. The hydrogel mixture combines polyethylene glycol diacrylate and gelatin methacrylate to improve mechanical stability, elasticity, and optical transparency. Several insert materials were tested, including a standard dissolvable material, gelatin, sugar, and isomalt. Simultaneously, a transparent, biocompatible bioreactor was designed via SolidWorks, fabricated using mSLA 3D printing from a biocompatible resin, and optimized through integration and leak testing. To address the challenge of interfacing the delicate hydrogel with rigid tubing, a novel coupling mechanism was developed, employing a mesh component that anchors the scaffold during hydrogel cross-linking.

Results: The main result was a transparent bioreactor system that enabled real-time visualization of flow through the engineered vessel scaffold. The optimized hydrogel composition improved scaffold stability while maintaining transparency for microscopic imaging. Isomalt was found to be the most suitable insert material, as it enabled the formation of a hollow structure with minimal interference during scaffold formation. Integration tests

demonstrated proper connection between the scaffold and the bioreactor, and the use of fluorescent beads confirmed the ability to observe flow, indicating the feasibility of visualizing fluorescent cells and fluorophores within the scaffold in future experiments. The connector allowed for easy integration between the scaffold and the bioreactor, supporting continuous flow while maintaining a leak-free environment.

Conclusions: This project demonstrates the feasibility of developing an accessible, transparent, and vessel-specific bioreactor for engineered blood vessel maturation and monitoring. The system combines a biocompatible hydrogel scaffold, controlled flow, and direct real-time imaging, and may serve as a foundation for an advanced platform for vascular tissue engineering.

Keywords: Bioreactor, Tissue Engineering, Engineered Blood Vessels, Hydrogel Scaffold.

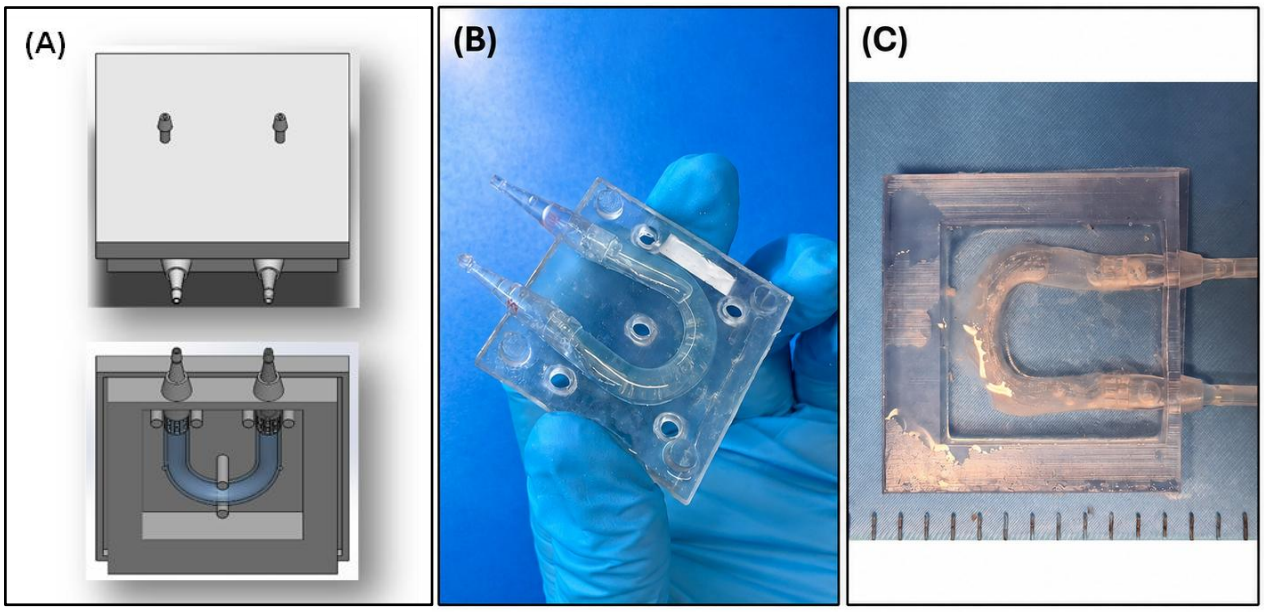

Figure 1: Design and assembly of the transparent vessel-specific bioreactor. (A) Schematic design of the bioreactor developed to support the engineered blood vessel. (B) U-shaped engineered vessel scaffold after photo crosslinking and cuff integration. (C) Assembled bioreactor system with the engineered vessel's scaffold.

Project 8

A Change of Heart: Navigating the Perception–Distortion Trade-Off In PPG-to-ECG Reconstruction

Aviv Neimann[1], Hadaya Aslan[1], Ido Turbiner[1], Oria Dudai[1], Shir Ben Meir[1], Doron Hanuka[1] Anat Rotschield[1] and Joachim Behar[1]

[1] Faculty of Biomedical Engineering, Technion – Israel Institute of Technology, Haifa, Israel

Introduction: Electrocardiography (ECG) is the gold standard for diagnosing cardiovascular diseases but requires dedicated clinical equipment, limiting its use for continuous monitoring. In contrast, photoplethysmography (PPG) is inexpensive, wearable, and widely available in consumer devices, but lacks clinically relevant morphological information. This project investigates deep-learning approaches for reconstructing ECG signals from PPG recordings while addressing the trade-off between numerical reconstruction accuracy and clinically meaningful signal quality.

Methods: We implemented a Dense Connected Bidirectional Long Short-Term Memory (DC-BiLSTM) model based on ReHeartNet and evaluated three training objectives: Mean Squared Error (MSE), Huber loss, and a composite loss combining Huber with CLEF perceptual regularization. Experiments were performed using the BIDMC PhysioNet dataset containing synchronized ECG and PPG recordings from 53 ICU patients. Signals were preprocessed using filtering, normalization, and phase alignment. Model performance was evaluated using distortion metrics (RMSE, PRD, Pearson correlation) together with rhythm and clinical metrics (Earth Mover's Distance, Kolmogorov-Smirnov statistic, Beat-Time MAE). Additional experiments investigated per-subject calibration and downstream pathology classification.

Results: Adding Huber loss produced only minor improvements over the original MSE objective. In contrast, incorporating CLEF perceptual regularization substantially improved both distortion and perceptual metrics. However, models trained using perceptual objectives exhibited an asymmetric perception-distortion trade-off during calibration. Distortion-trained models consistently improved regardless of calibration objective, whereas perception-trained models degraded when calibrated using distortion-based losses. Furthermore, calibrating each model using only 100 seconds of subject-specific data significantly improved reconstruction quality, particularly for rhythm preservation and downstream pathology classification.

Conclusions: Our findings demonstrate that ECG reconstruction from wearable PPG signals benefits substantially from subject-specific personalization. The discovered asymmetry in the perception-distortion trade-off suggests that optimization objectives strongly influence calibration behavior and generalization performance. These insights may contribute to future wearable systems capable of continuous cardiovascular monitoring and earlier disease detection through personalized ECG reconstruction.

Keywords: Photoplethysmography, Electrocardiography, Deep Learning, Wearable Monitoring.

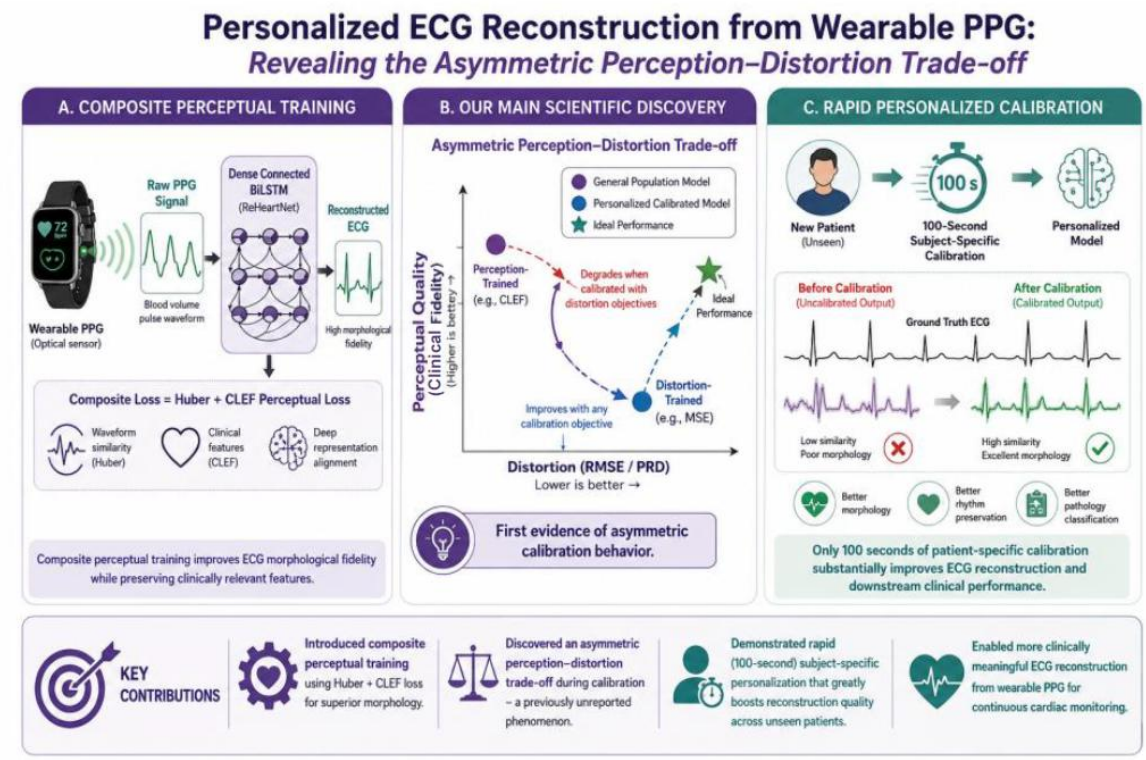

Figure 1: *Graphical overview of the proposed personalized PPG-to-ECG reconstruction framework.*

Project 9

Real-Time Gait Asymmetry Detection in Transtibial Amputees

Yarin Aunallah[1], Hala Majdoub[1], Razan Mousa[1], Mysan Nassar[1], Amjad Okasha[1], Raz Margi[1], Bar Kiner[1], Daniel Katz[1] and Arielle Fischer[1]

[1] Faculty of Biomedical Engineering, Technion – Israel Institute of Technology, Haifa, Israel

Introduction: Gait asymmetry is a common problem in individuals with transtibial amputation and may increase uneven joint loading, compensatory movement patterns, and walking effort. Conventional gait analysis is usually performed in dedicated laboratories and often provides results only after data collection. The objective of this project was to develop a wearable, real-time system that detects gait asymmetry and provides vibrotactile feedback while walking.

Methods: The system uses two wearable sensors placed on the shanks to allow direct comparison between the right and left limbs. Sensor data are transmitted to a control unit located on a waist belt, which also contains the vibration feedback unit, as presented in Figure 1. The algorithm was evaluated using 65 walking trials collected from 10 participants, including 30 normal walking trials and 35 simulated limping trials. In addition, a pilot trial was conducted with a former soldier who had a below-knee fixation device on his left leg following a service-related injury.
For each gait cycle, the algorithm identifies the mid-swing peak, searches for toe-off before it and heel-strike after it, calculates the swing time of each leg, and computes a swing-time-based symmetry index. A sliding symmetry index is then calculated using five consecutive swing-time values. When the calculated asymmetry exceeds the selected threshold, a vibration cue is activated on the belt.

Results: Normal walking produced very low symmetry index values, approximately 0-1.6%, indicating similar swing times between the legs. In contrast, simulated limping produced substantially higher symmetry index values, approximately 63-79%, indicating clear gait asymmetry. In the pilot trial with the injured participant, the system detected approximately 12% asymmetry, although the asymmetry was not clearly observed. This suggests that the system may identify mild asymmetry in addition to severe gait deviations. The sliding symmetry index remained low during normal walking and stayed above the selected threshold during asymmetric walking. Visual comparison between the walking videos and sensor signals also supported the correct detection of the main gate events.

Conclusions: This project demonstrates a wearable closed-loop prototype for real-time gait asymmetry monitoring and vibrotactile feedback. The system integrates sensing, processing, decision-making, feedback, and mechanical design into a practical platform that may support gait training outside a traditional gait laboratory.

Keywords: gait asymmetry, transtibial amputation, wearable sensors, vibrotactile feedback

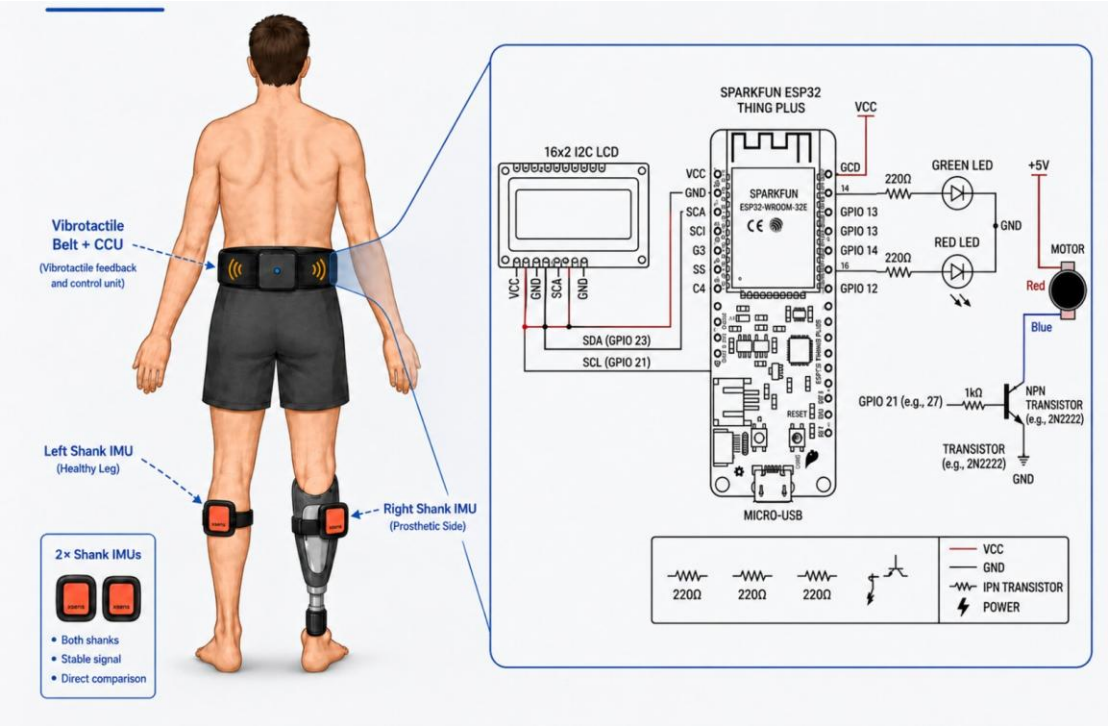

Figure 1. Schematic representation of the wearable gait-monitoring device. *The figure presents a rear view of a user wearing two sensors and a waist belt containing the control unit. A zoomed callout from the belt shows the internal layout of the control unit, including the microcontroller, display, indicator lights, vibration motor driver, and main wiring connections. Labels and arrows highlight the sensor placement on both legs, the waist-mounted feedback unit, and the electronic components inside the control unit.*

Project 10

Non-Invasive Multimodal Imaging of LPS-Induced Inflammation in a 3D Bone Marrow Model

Ghina Abu Hable[1], Jonel Daud[1], Haide Garzuzi[1], Deema Ghanem[1], Mays Khalil[1], Yasmin Khazim[1], Doaa Ali Naffaa[1], Narmeen Haj[1], Amit Parizat[1] and Katrien Vandoorne[1]

[1] Faculty of Biomedical Engineering, Technion – Israel Institute of Technology, Haifa, Israel

Introduction: Inflammatory activation of bone marrow cells is a key feature of sepsis and other immune disorders. However, conventional two-dimensional cultures fail to reproduce the structural and mechanical cues of the native bone marrow niche, whereas animal models offer limited experimental control. This project aimed to develop a controllable three-dimensional bioprinted bone marrow model that supports primary hematopoietic cells and enables non-invasive monitoring of lipopolysaccharide (LPS)-induced inflammation.

Methods: Bone marrow cells were isolated from mouse femurs and tibias, processed into single-cell suspensions, enriched for hematopoietic stem and progenitor cells (HSPCs), and characterized by flow cytometry. To establish reporter-based imaging, CT26 murine colon carcinoma organoids were transduced using either the conventional lentiviral transduction method or the MISSION® Lentiviral Packaging Mix. Two reporter systems were evaluated: green fluorescent protein (GFP) and the mouse sodium iodide symporter (mNIS) for fluorescence and single-photon emission computed tomography (SPECT) imaging, and red fluorescent protein (RFP) together with chemical exchange saturation transfer (CEST) for fluorescence and future magnetic resonance imaging (MRI). Technetium-99m uptake was assessed by SPECT to evaluate the feasibility of mNIS-based nuclear imaging. In parallel, collagen methacryloyl (ColMA) hydrogel constructs were bioprinted, crosslinked and seeded with cells to establish preliminary three-dimensional scaffolds for future LPS-induced inflammation studies. An anatomically relevant femur-shaped scaffold was also fabricated using a sacrificial mold and evaluated for cell attachment and localization.

Results: The bone marrow isolation protocol generated a viable, low-aggregation cell suspension suitable for downstream enrichment and bioprinting. Flow cytometry confirmed successful enrichment of the target HSPC population. Reporter validation demonstrated comparable GFP expression between the conventional lentiviral transduction method and the MISSION® Packaging Mix, whereas conventional lentiviral transduction produced stronger RFP expression and was selected for subsequent experiments. SPECT imaging detected technetium-99m uptake in mNIS-expressing organoids, demonstrating the feasibility of nuclear reporter-based imaging. In parallel, bioprinted ColMA constructs maintained their three-dimensional architecture after crosslinking and supported cell incorporation, while the femur-shaped scaffold enabled successful cell attachment and localization.

Conclusion: This project established the biological, imaging and biofabrication framework for developing a reproducible, non-invasively imageable three-dimensional bone marrow model. The platform provides a controlled in vitro system that bridges conventional cell culture and

animal models and may support future studies of LPS-induced inflammation, multimodal imaging and therapeutic evaluation.

Keywords: Hematopoietic stem cells, Bone Marrow Niche, Fluorescent reporters, Multimodal Imaging.

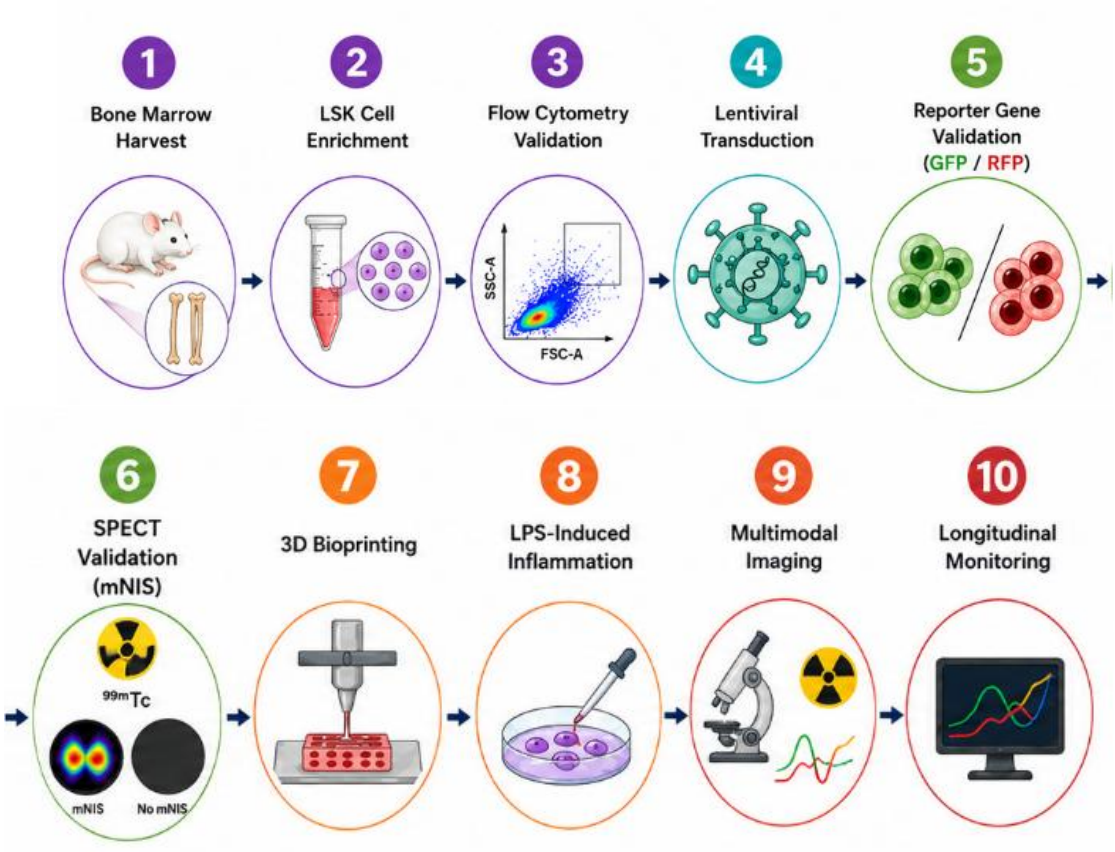

Figure 1. *Overview of the experimental workflow for developing and validating the 3D bioprinted bone marrow platform.*

Project 12

Effects of Microtoxicity on Heart Rate Variability Patterns in Zebrafish

Mohamad Abu Raiya[1], Natalie Atias[1], Lama Farah[1], Michel Laskin[1], Meital Sabatan[1], Riyad Zoubi[1], Nir Almog[1], Layan Hamed[1], Anat Rotschield[1] and Yael Yaniv[1]

[1] Faculty of Biomedical Engineering, Technion – Israel Institute of Technology, Haifa, Israel

Introduction: Early detection of toxicity with regards to both low doses and short exposure times remains challenging because conventional diagnostic methods are usually invasive and often identify toxicity only after physiological damage has already occurred. This project aims to develop a non-invasive computational framework capable of identifying such early microtoxicity by analyzing changes in heart rate variability patterns in zebrafish larvae. The long-term objective is to establish a methodology that may support future real-time toxicity monitoring in human health applications.

Methods: Cardiac activity was recorded non-invasively in transgenic zebrafish larvae expressing green fluorescent protein in the cardiac muscle using optical imaging. A tailored signal-processing pipeline was developed to preprocess the recordings, detect heartbeats, calculate beat-to-beat intervals, and extract quantitative features describing the underlying heart rate variability patterns within the data. Features from the time, frequency, and non-linear domains were used to train a Temporal Convolutional Network for toxicity classification. The model optimized for several pharmaceuticals in separate, each with its own dataset: it was first validated using pharmacological datasets at multiple concentrations and subsequently evaluated using larvae exposed to Terfenadine at multiple concentrations and exposure durations.

Results: The developed framework successfully distinguished between control, low-risk, and high-risk toxicity conditions based on heart rate variability patterns. The strongest performance was achieved for the Terfenadine dataset, where the model correctly identified most microtoxicity cases while maintaining clear separation between healthy and severely affected larvae.

Conclusions: This study demonstrates that our pipeline of non-invasive analysis of heart rate variability, combined with signal processing and deep learning, provides a promising approach for microtoxicity detection in zebrafish. Here we establish a foundation for future research involving larger datasets and additional toxic compounds that may ultimately contribute to wearable technologies for continuous, real-time toxicity monitoring in humans.

Keywords: Deep Learning, Heart Rate Variability, Microtoxicity Detection, Zebrafish

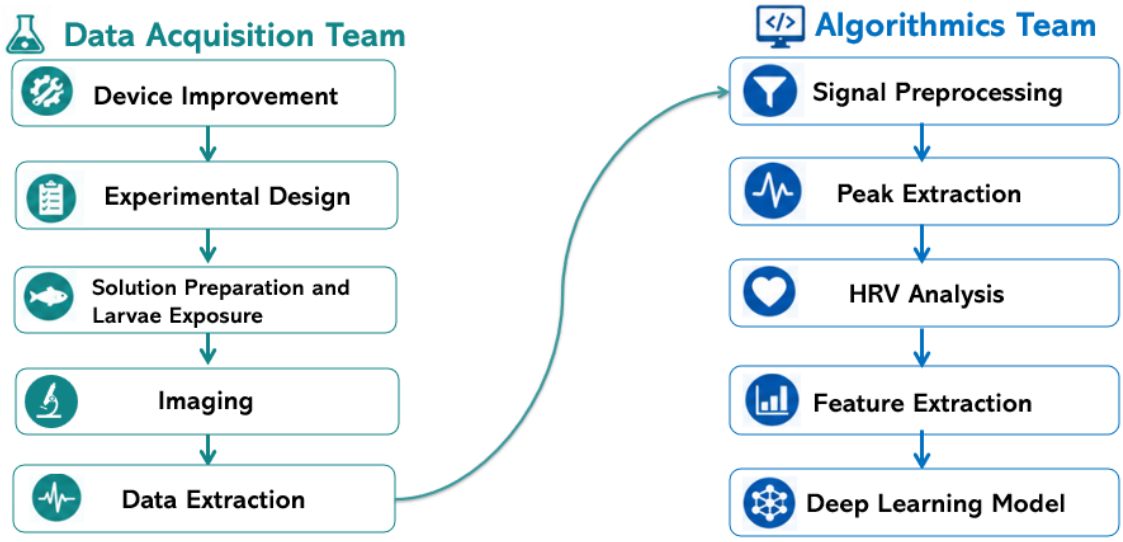

Figure 1 *- Overview of the micro-toxicity detection framework.*

Project 14

Development and Evaluation of Dye-labeled Nanoparticles for Enhanced Trametinib Solubility and Ocular Delivery

Lian Hamza[1], Naama Yaffa[1], Shada Shalata[1], Suzanne Kayal[1], Tal Levy[1], Tasnim Hasi[1]. Amir Shagoury[1], Amit Parizat[1] and Yossi Shamay[1].

[1] Faculty of Biomedical Engineering, Technion – Israel Institute of Technology, Haifa, Israel

Introduction: Age related macular degeneration involves pathological retinal blood vessel growth, currently treated via invasive ocular injections with low patient compliance. Noninvasive topical alternatives are urgently needed but remain severely limited by ocular barriers and the extremely poor water solubility of antiangiogenic drugs. To directly address this solubility challenge and overcome physical barriers, this project develops a novel nanoparticle formulation combining an antiangiogenic drug, a functional dye, and a stabilizing polymer.

Methods: Sequential screening workflow selected the optimal drug and dye based on physical properties. Nanoparticles were formulated via spontaneous self-assembly nanoprecipitation. Formulations were evaluated for size and uniformity using dynamic light scattering, and drug encapsulation was quantified via high performance liquid chromatography. Biological activity was assessed in endothelial cell models, and ocular delivery potential was evaluated using a custom mucin-based barrier penetration assay.

Results: Initial screening demonstrated the platform's ability to overcome drug insolubility, increasing Cabozantinib aqueous solubility by 287-fold. Following biological evaluation, Trametinib showed the most consistent antiangiogenic activity and was selected as the lead therapeutic agent. Indocyanine green was chosen as the lead dye for its superior clarity and uniformity. Adding polyvinyl alcohol-maintained particle size below one hundred and fifty nanometers and prevented aggregation. Ultimately, the final nanoparticles achieved a 325-fold increase in Trametinib solubility, preserved their antiangiogenic activity in endothelial cells, and demonstrated enhanced penetration through a simulated mucin barrier compared to non-stabilized formulations.

Conclusions: This nanoparticle platform successfully addresses drug insolubility and demonstrates enhanced penetration across an in vitro model of the initial ocular barrier while preserving its antiangiogenic activity. These findings highlight its potential as a platform for noninvasive topical drug delivery in age-related macular degeneration. Further studies are required to evaluate diffusion across additional ocular barriers and validate its performance in advanced biological models.

Keywords: Nanomedicine, Macular Degeneration, Ocular Drug Delivery, Antiangiogenic Therapy.

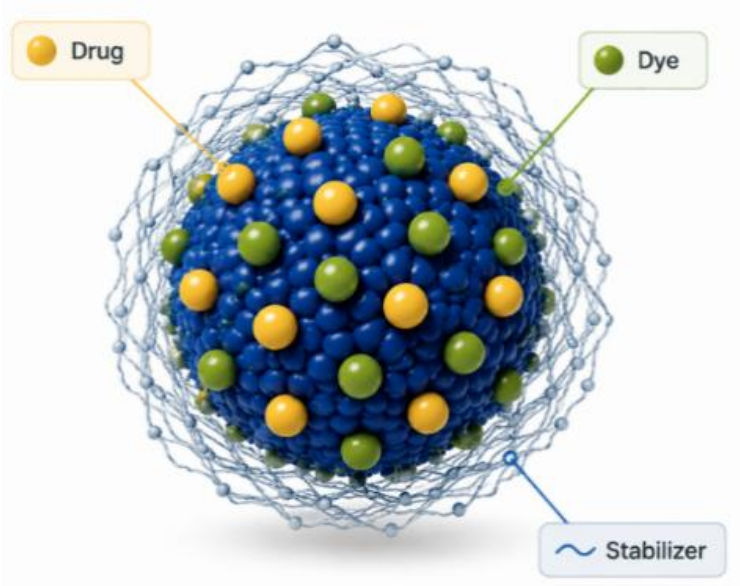

***Figure 1**: Illustration of our platform: nanoparticle of drug, dye and stabilizer.*

Project 15

Soft and Flexible Device for Leadless Bioelectronic Modulation

Nagham Aga[1], Deema Badran[1], Lea Benabou[1], Bessie Formigoni[1], Nir Marcusohn[1], Noam Pahima[1], Layan Habib[1], Shirley Yitzhak-David[1], Amit Parizat[1] and Menachem (Hemi) Y. Rotenberg[1]
[1] Faculty of Biomedical Engineering, Technion – Israel Institute of Technology, Haifa, Israel

Introduction: Peripheral nerve injuries require prolonged rehabilitation, conventionally treated via electrical stimulation. However, traditional metal leads and rigid silica fibers introduce a severe mechanical mismatch with soft tissues, causing chronic inflammation and implant failure. Optogenetics offers wire-free alternatives but remains clinically limited due to genetic modification requirements. To bridge these mechanical and clinical gaps, this project develops a soft, wireless, and biocompatible optoelectronic interface. By combining a wireless porous silicon diode, which converts light to electrical stimulation, with a flexible soft optical fiber, we eliminate the need for physical wires.

Methods: We fabricated three distinct core-cladding fiber configurations: Polyvinyl Alcohol (PVA), Polydimethylsiloxane (PDMS) with Polyacrylamide (pAAm), and Alginate-pAAm, optimizing protocols to minimize optical scattering and attenuation. Core-cladding boundaries were verified using brightfield and confocal microscopy. Refractive indices were measured using a digital refractometer to calculate the Numerical Aperture (NA), and optical attenuation was evaluated under 640 nanometers laser illumination. Uniaxial tensile testing extracted Young's modulus and maximum strain (elasticity). Additionally, patch-clamp recordings under 625 nanometers illumination validated the porous silicon membrane's photoelectric effect and oxygen plasma activation efficiency.

Results: Microscopy confirmed successful core-cladding boundary formation. Refractive index measurements confirmed $n_{core} > n_{cladding}$ for all fibers. Calculated NAs fell within standard hydrogel limits (0.1–0.5), with PDMS-pAAm yielding the highest NA (0.46) and Alginate-pAAm the lowest (0.18). Optical characterization via Laser attenuation testing revealed low attenuation coefficients for PVA (0.4 decibels per centimeter) and PDMS-pAAm (0.48 decibels per centimeter), whereas Alginate-pAAm exhibited high attenuation due to concentration-dependent turbidity. Testing the PDMS core without cladding resulted in significantly higher attenuation, proving cladding necessity. Patch-clamp characterization of the silicon membrane confirmed a robust photoelectric response with peak currents reaching 80 nanoamperes, demonstrating enhanced charge generation following oxygen plasma activation.

Conclusions: We demonstrated the feasibility of fabricating customized, soft optoelectronic interfaces with tailored properties. Rather than finding a single universal material, we established a versatile library of functional soft optical fibers: biodegradable PVA offers high elasticity; bio-inert PDMS-pAAm provides superior transparency and high NA; and Alginate-pAAm uniquely incorporates a tissue-friendly natural biopolymer. This material-matching approach allows customization of bioelectronic interfaces to meet diverse physiological and mechanical demands.

Keywords: biocompatible optical fibers, porous silicon bioelectronics, nerve stimulation, core-cladding fabrication.

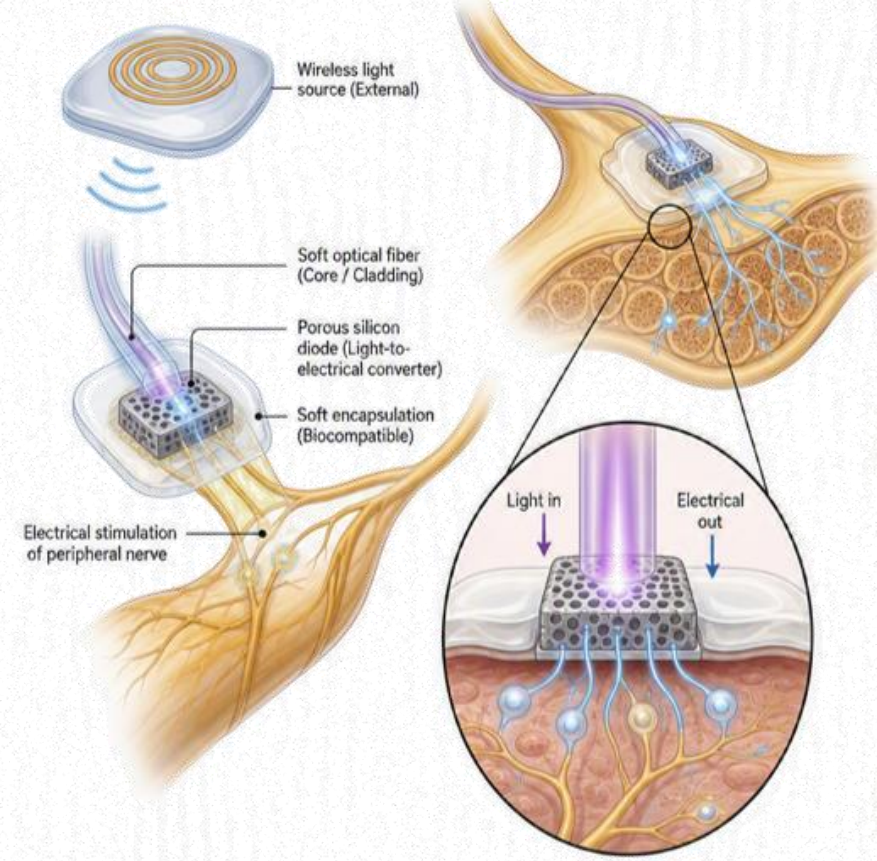

Figure 1. *Operational mechanism and tissue integration of the wireless soft optoelectronic interface. Schematic overview showing the external light source, the customized core-cladding soft optical fiber, and the soft-encapsulated porous silicon diode delivering leadless electrical stimulation to the peripheral nerve.*

Project 17

Real-Time and Cost-Effective Three-Dimensional Cavitation Localization Using a Hybrid Arrival-Time and Beamforming Approach

Or Ben Israel[1], Mike Krayani[1], Nir Mikel[1], Tamar Naigertsik[1], Yarden Vanun[1], Michal Moshe[1], Alon Remer[1], Amit Parizat[1] and Avinoam Bar-Zion[1]

[1] Faculty of Biomedical Engineering, Technion – Israel Institute of Technology, Haifa, Israel

Introduction: Focused ultrasound is a non-invasive therapeutic technique that concentrates acoustic energy at a precise target deep within tissue and is increasingly used for neurological treatments. Its effect is closely tied to cavitation, the oscillation and violent collapse of microscopic bubbles under the acoustic field, which may damage healthy tissue when occurring outside the intended target. Current clinical tools either detect cavitation without localization or provide localization at the cost of hundreds of sensors and high computational load. Therefore, this project aims to combine these two approaches into a hybrid system that provides accurate three-dimensional cavitation localization in real time and at low cost.

Methods: An imaging pulse modulated on a continuous therapeutic wave was designed, simulated, and transmitted using a hemispherical transducer array through a computed-tomography-modeled skull, then the received signals undergo frequency-domain filtering isolating the imaging-band signal for further processing at each sensor. A coarse three-dimensional position estimate was obtained from arrival-time differences using iterative outlier rejection before position solving. A 10^3 mm^3 region of interest was built around this estimate and refined using a delay-and-sum energy-mapping algorithm. In parallel, bench experiments used a real transducer and a passive sensor to record acoustic signals from laboratory-generated microbubbles in a water tank, to characterize the cavitation signal, including its harmonic content and harmonic signal-to-noise ratio.

Results: The coarse arrival-time-based estimation kept the localization error below 5 mm across most tested source locations, ensuring that the resulting region of interest reliably contained the true source position for the subsequent refinement stage. Combining this estimate with the region-of-interest beamforming refinement, the hybrid system achieved a localization error of 1.58 ± 1.84 mm across 18 tested source locations, using only 64 evenly distributed sensors, with no accuracy gain from additional sensors. The combined pipeline produced a location estimate in a mean of 2.68 ± 0.28 seconds across the same 18 runs. Independently, bench experiments recorded the returning microbubble signal in real time, and frequency-domain analysis confirmed the expected harmonic content and quantified its signal-to-noise ratio.

Conclusions: These results demonstrate that a hybrid approach, relying on only a small subset of sensors from the existing clinical system, can achieve sufficient accuracy to support clinical decision-making. Its fast runtime further supports the system's potential for real-time integration into clinical focused ultrasound monitoring.

Keywords: Focused Ultrasound Therapy; Cavitation Localization; Passive Acoustic Mapping; Beamforming;

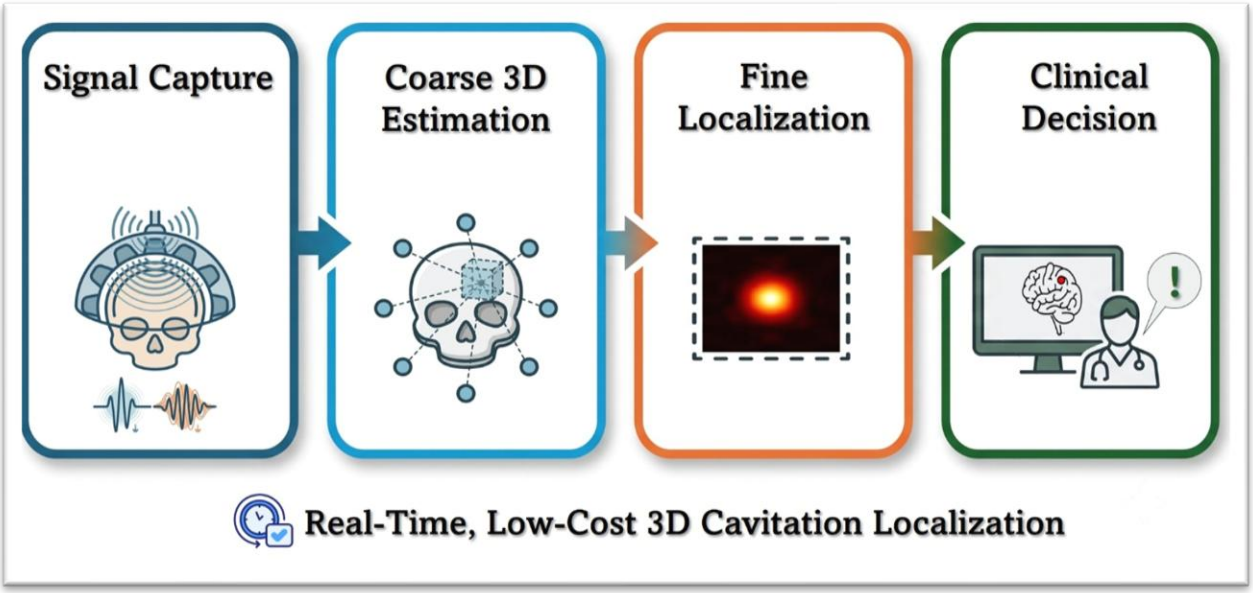

Figure 1. *Overview of the hybrid Arrival-Time-Beamforming pipeline for real-time, low-cost 3D cavitation localization: the sensor array captures the imaging pulse and its echo → arrival-time differences yield a fast, coarse 3D position estimate → delay-and-sum beamforming refines this estimate to sub-millimeter precision within a focused region of interest → the result enables real-time clinical feedback during focused ultrasound treatment.*

Project 18

Innovative Solutions for Anchoring Cardiovascular Devices: Preventing Migration and Enhancing Stability

Dan Barabash[1], Maria Aweda[1], Rima Fisel[1], Vivian Salem[1], Zina Taha[1], Tirosh Mekler[1], Yevgeniy Kreinin[1], Daniel Katz[1] and Netanel Korin[1]

[1] Faculty of Biomedical Engineering, Technion – Israel Institute of Technology, Haifa, Israel

Introduction: Transcatheter mitral valve replacement is a minimally invasive alternative for patients with severe mitral valve disease who are ineligible for open heart surgery, but secure anchoring of the replacement valve remains a major clinical challenge. The native mitral annulus has an irregular, non-circular shape that does not conform well to the rigid frames used in current devices, causing inadequate anchoring, valve migration, and leakage of blood around the valve. The objective of this project was to design and evaluate a sealing interface wrapped around a transcatheter framework to improve mechanical friction, optimize structural engagement with surrounding tissue, and ultimately prevent device displacement and paravalvular leakage.

Methods: All system components were designed using computer-aided design and fabricated using three-dimensional printing. The housing was printed from polylactic acid; within it, a compliant annulus model was cast from silicone elastomer using two independent patient-derived geometries reconstructed from computed tomography scans, tested under varying calcification conditions simulated using embedded rigid inclusions. The valve was modeled as a disc printed from thermoplastic polyurethane: a rigid control disc with full internal infill, and a deformable disc with a rigid core and an unfilled compliant rim allowing it to conform to the annulus. Each configuration was evaluated in at least three replicates via push-out testing on a tensile testing machine. Comparisons were made per patient model and calcification level using independent-samples Welch t-tests. Additionally, in the first model, solution effect, defined as solution mean push-out force minus control mean push-out force was compared across three calcification levels using bootstrap-based pairwise comparisons with Holm–Bonferroni correction.

Results: Across two independent patient-derived annulus models, the deformable disc produced higher push-out force than the rigid control in every condition, with improvements ranging from 3% to 33% depending on calcification level. The largest, statistically significant improvements occurred under calcification: +15.6% under low calcification and +32.5% under high calcification in the first model, and +13.5% under high calcification in the second model. Improvements without calcification were smaller and not statistically significant. The solution effect increased across calcification levels, indicating that the deformable rim provided greater benefit as annular calcification and geometric mismatch increased.

Conclusions: This work provides proof of concept that a compliant sealing geometry increases anchoring force in a transcatheter mitral valve replacement system. The benefit is consistent across two patient-specific anatomies and reaches significance under tissue calcification precisely where the design offers the greatest clinical value. These findings support continued

development of geometry-adaptive sealing strategies, including alternative materials and catheter-compatible designs, for improving anchoring stability and reducing valve migration and paravalvular leakage.

Keywords: transcatheter mitral valve replacement, Tissue-mimicking silicone elastomer, adaptive sealing interface, push-out force testing

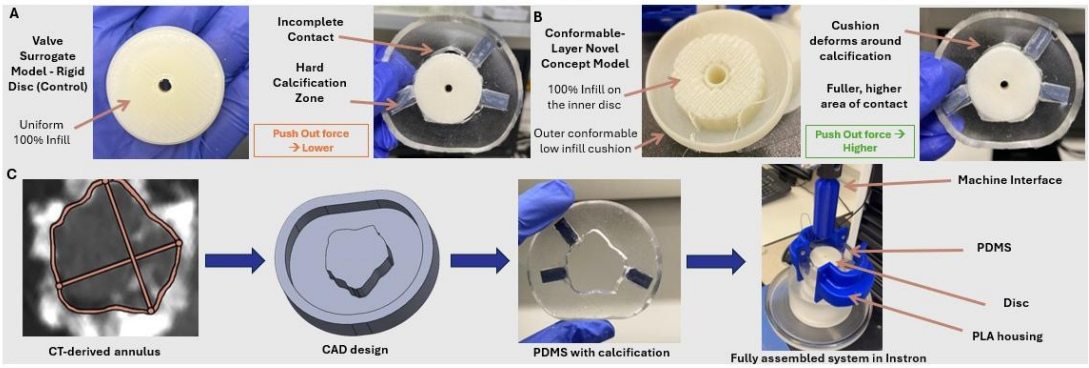

***Figure 2: Disc design and experimental pipeline**. (A) Rigid control disc: full infill, incomplete contact with calcification, lower push-out force. (B) Deformable interface: compliant outer cushion conforms around calcification, higher push-out force. (C) Fabrication and testing: CT-derived geometry, CAD design, PDMS casting, and the assembled system on Instron.*

Project 19

Real-Time fMRI Brain Activation Monitoring

Adi Sasson[1], Gal Ben Or[1], Elad Fonia[1], Roi Kipper[1], Elia Haj[1], Elodie Haggiag[1], Anat Rotschield[1], Marwan Bebar[1], Dalia Braverman-Jaiven[1], Rola Farah[1] and Tzipi Horowitz-Kraus[1]

[1] Faculty of Biomedical Engineering, Technion – Israel Institute of Technology, Haifa, Israel

Introduction: Standard functional MRI (fMRI) analysis is retrospective - researchers wait days to weeks for offline post-processing. By then, unusable data cannot be reacquired, meaning wasted scanner time and delayed research. Real-time fMRI addresses this by giving immediate feedback during the scan, letting operators catch motion artifacts or poor task performance while the participant is still in the scanner. Existing tools, however, are often costly, proprietary, or infrastructure-heavy, beyond many laboratories' reach. This project develops and validates a free, accessible real-time fMRI system that computes and displays reliable brain-activation maps live, open to any research laboratory.

Methods: The standard offline preprocessing pipeline (motion correction, co-registration, segmentation, normalization) was optimized into a concurrent, low-latency architecture that delivers near-real-time activation estimates from cumulative partial data rather than a single end-of-session batch. Task-related activation was estimated with GLM, mapping the block design onto the acquired signal. For validation, output was benchmarked against a gold standard using a data-driven task-related auditory cortex mask built from ICA of over 100 offline story-listening scans. Live single-subject activation maps were projected onto an age-stratified reference distribution. An MRI simulator, which streams acquired scan data to test and validate the pipeline offline, was developed.

Results: GLM-derived outputs localized the task activation to bilateral auditory cortex in live subjects' scans, matching the expected story-listening response. Task-specificity was further confirmed against a control condition - a five-minute run with no story - visually validated by the lab's researchers. Subject movement detection was validated via live scans. The pipeline was substantially faster than SPM (existing processing protocol) at every stage, cutting per-run processing from ~50 min to ~5 min (scan length). Informative results are updated every 20 sec throughout the scan. Correlating each subject's real-time and SPM maps gave a moderate positive distribution (mean Pearson r = 0.49). Live projection onto the age-dependent reference distribution was feasible in real time, though that age–activation relationship was sparse.

Conclusions: By combining offline-grade accuracy with an average ten-fold reduction in processing time, this free, openly accessible tool gives laboratories reliable brain-activation results in real-time. Its low barrier to adoption and rapidity make it a practical, novel alternative to costly proprietary real-time fMRI processing software, enabling live activity and movement monitoring in the scanner room. Looking ahead, we aim to expand to a range of research tasks and evaluate our product on a wider range of subjects.

Keywords: Real-Time-fMRI, Accessible Neuroimaging Tool, Brain Activation Monitoring

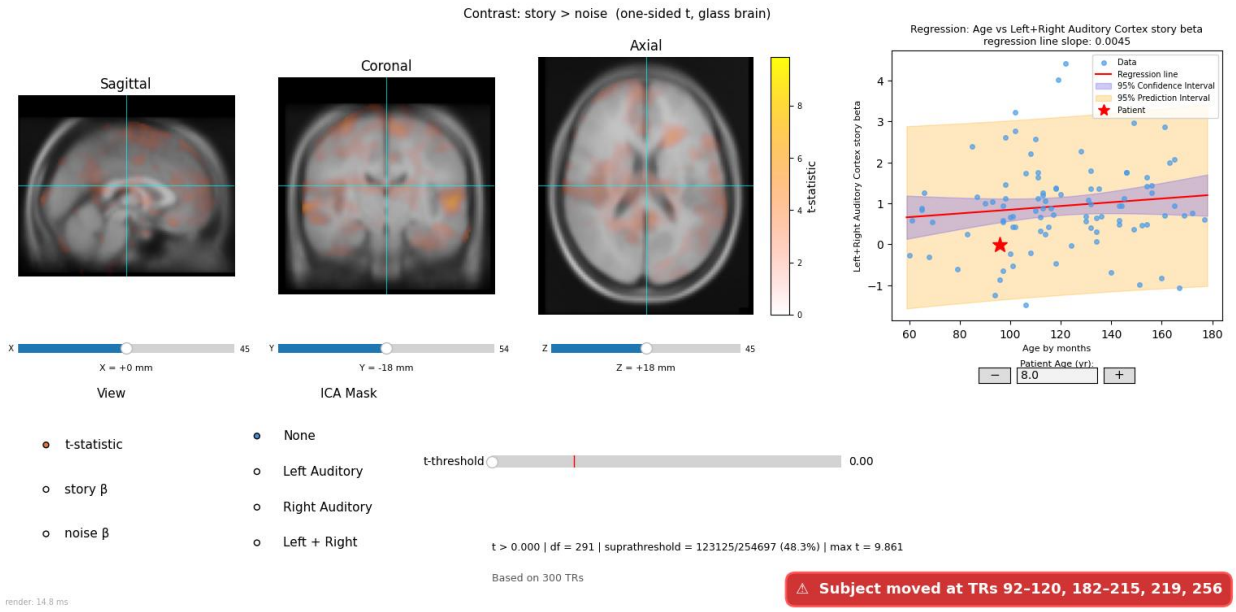

Figure 1. *Real-time activation-monitoring dashboard generated live during scanning. Top-Left: Glass-brain activation maps (sagittal, coronal, axial) for the story > noise contrast. Top-Right: The current subject's real-time auditory-cortex activity (red star) projected onto the age-stratified normative reference distribution. Bottom-Right: Motion detection alert.*

Project 21

Innovative Solutions for Control and Sensation in Upper-Limb Prosthetics

Liad Katzir[1], Nadav Cohen[1], Nofar Shechter[1], Rand Armaly[1], Taly Chiche[1], Daniel Katz[1], Yaacov Melinovich[2], Uzi Shudron[2]

[1] Faculty of Biomedical Engineering, Technion – Israel Institute of Technology, Haifa, Israel
[2] Haifa3D Non-Profit Organization

Introduction: Most modern commercial upper-limb prosthetics lack sensory feedback and rely on muscle activation\ are held on the stump, which can trigger phantom limb pain and force users to rely on constant visual tracking. The objective of this project is to develop a closed-loop system that provides non-stump-based activation alongside reliable sensing and haptic feedback mechanisms. The system aims to restore the sensation of touch, reduce cognitive load, and enable more natural control and grasping.

Methods: The proposed system architecture is based on four modules that together form a closed loop of activation and feedback. For prosthetic activation, the design integrates two activation technologies: the first relies on surface electromyography (EMG) sensors located on the shoulder to control the opening and closing of the prosthetic. The second utilizes dual inertial measurement units (IMU) on the arm and residual limb to calculate relative motion and accurately detect the user's intent to rotate the wrist. For the sensing and feedback array, the system was designed to embed force-sensitive resistors (FSR) and piezoelectric sensors (PVDF) in the prosthetic's fingertips. According to the design, these data are processed to provide two types of feedback delivered to the user's arm: 'slip feedback', which combines data from both sensor types to detect slip vibrations and translates them into a skin-stretch sensation, and 'pressure feedback', which uses the force sensor data to control electric motors that apply proportional physical pressure to the arm. Additionally, the system's algorithm features an autonomous locking mechanism, designed to use the fingertip sensor data to automatically lock the grasp once a stable, slip-free grip is detected.

Results: The primary success was achieved in the implementation of the pressure feedback system: the system, which included a glove with five force-sensitive resistors (FSR), successfully and linearly translated static grip strength into the activation of electric motors on the user's arm. False activations caused by electromagnetic noise were effectively resolved by upgrading the noise-filtering algorithm, and the motor rotation direction issue was successfully corrected through mechanical adjustment. The system provided an accurate proportional relationship between the pressure sensed at the fingertips and the pressure applied to the arm. Conversely, testing of the shoulder activation module revealed that the tested electromyography (EMG) sensor was overly sensitive to environmental noise and movement. This sensitivity caused rapid signal saturation and false activations during rest, indicating that the specific component is insufficiently stable for practical use and requires a more isolated alternative. Due to time constraints, the remaining modules described in the architecture did not reach the physical development and testing phase.

Conclusions: This project demonstrated the feasibility of a pressure-based feedback system that transmits touch sensations directly to the user's arm. While pressure feedback yielded encouraging results, proving that grip force can be translated into intuitive tactile sensations, the activation module highlighted that electromyography-based control requires industrial-grade, shielded hardware to ensure reliable operation. Future work will focus on optimizing mechanical interfaces and integrating advanced activation sensors to enhance overall system reliability.

Keywords: Upper-limb prosthetics, Haptic feedback, Sensory substitution, Electromyography

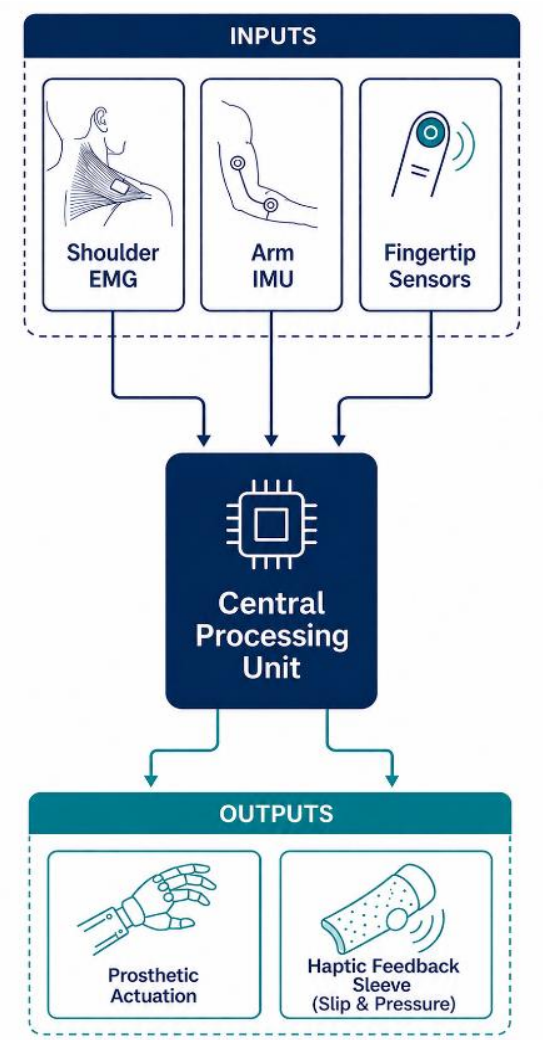

Figure 1: *Flow diagram of the proposed closed-loop prosthetic system architecture.*

Project 30

Investigating Electrical Behavior in Nanofluidic Channels Through Numerical Modeling and Experimental Validation

Yarin Dvir[1], Hagar Hamburger[1], Astar Kakoon[1], Yasmin Tchigevsky[1], Ivy Bhattacharya[1], Marzia Iarosi[1], Amit Pariza[1]t and Amit Meller[1]

[1] Faculty of Biomedical Engineering, Technion – Israel Institute of Technology, Haifa, Israel

Introduction: The Meller Laboratory develops nanofluidic channels for real-time characterization of biological particles. Reliable prediction of the electric field inside nanochannels is essential for interpreting particle transport and electrokinetic experiments. Previous experiments revealed inconsistent particle behaviours that could not be fully explained by the theoretical model, suggesting that one or more simplifying assumptions might be incomplete or invalid. In this work, the physical assumptions underlying the electrical behaviours of the nanochannel were systematically examined using a physics-based numerical model to identify the source of the observed discrepancies.

Methods: A three-dimensional finite element model of the nanochannel was developed in COMSOL Multiphysics to simulate the electric field distribution. The model incorporated the complete multilayer device geometry and the electrical properties of the electrolyte and surrounding materials. The influence of the material layers and channel T-junctions on the electric field was investigated numerically. A parallel-resistor conductance model was then formulated to distinguish bulk and surface contributions to the total conductance and to guide concentration-dependent current-voltage measurements. Finally, the numerical predictions were compared with the experimental measurements over a range of sodium chloride concentrations.

Results: The simulations demonstrated that the surrounding material layers have a negligible influence on the electric field inside the nanochannel, while T-junctions introduce only localized perturbations that rapidly decay away from the junction region. Following this step the imaging point was distanced from the T-junction. Based on the resistor model, a concentration-dependent conductance experiment was proposed to separate bulk and surface contributions. The experimental measurements indicated that surface conductance is negligible, while the measured bulk conductance exceeded the theoretical prediction. This discrepancy was ultimately attributed to fabrication-related ionic contamination. Following the updated fabrication protocol, the experimental conductance showed good agreement with the numerical predictions.

Conclusions: By systematically evaluating the underlying physical assumptions, the combined numerical and analytical framework identified bulk conductivity, rather than electric field non-uniformity or surface conductance, as the primary source of the observed experimental discrepancies. Following improvements to the fabrication protocol, the validated model provides a useful framework for interpreting electrokinetic experiments, supporting nanochannel design, and guiding future investigations of electrical transport phenomena in nanofluidic systems.

Keywords: Nano-Channel, Finite-Element Numerical Simulation, Bulk Conductance.

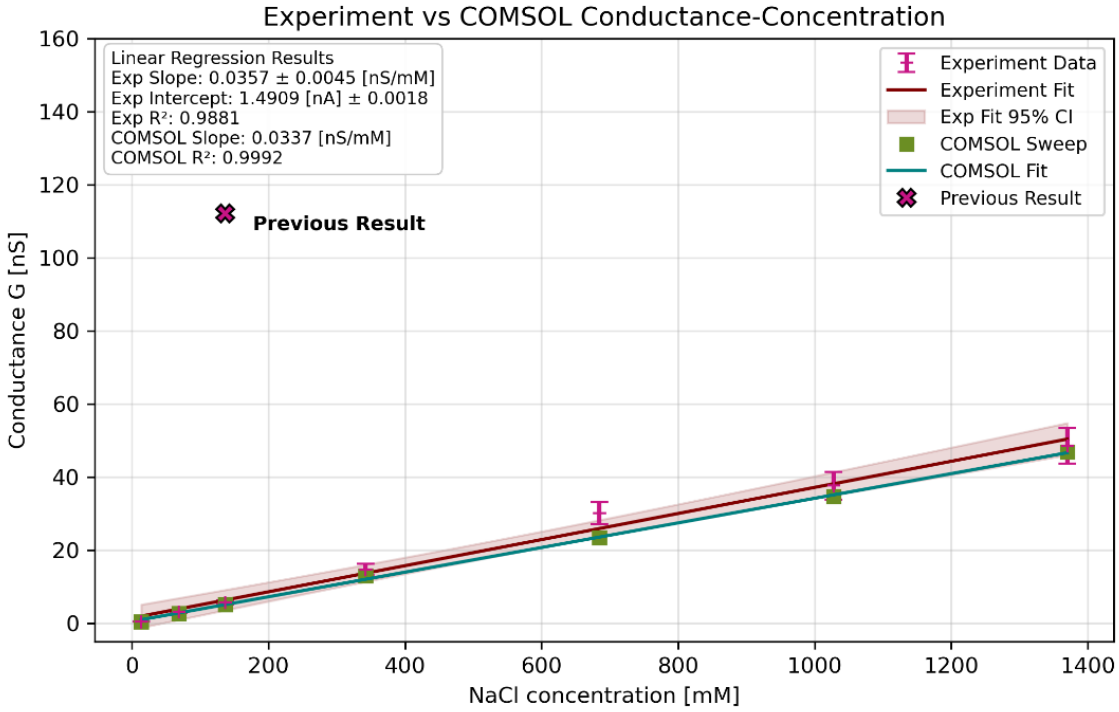

Figure 1. *Comparison between experimental measurements and COMSOL Multiphysics simulations of total channel conductance as a function of bulk solution concentration. Experimental results are shown in pink, while COMSOL parametric sweep results over different concentrations are shown in green, together with their corresponding linear fits. The "x" marker represents a previous experimental measurement, highlighting the discrepancy observed before the fabrication protocol update. The legend includes the linear fit equations and statistical parameters for both datasets.*